Central Lancashire Online Knowledge (CLoK)

Title	MIP-based electrochemical protein profiling
Type	Article
URL	https://clok.uclan.ac.uk/13789/
DOI	https://doi.org/10.1016/j.snb.2014.07.100
Date	2014
Citation	Bueno, Lígia, El-Sharif, Hazim F., Salles, Maiara O., Boehm, Ryan D., Narayan, Roger J., Paixão, Thiago R.L.C. and Reddy, Subrayal M orcid iconORCID: 0000-0002-7362-184X (2014) MIP-based electrochemical protein profiling. Sensors and Actuators B: Chemical, 204. pp. 88-95. ISSN 0925-4005
Creators	Bueno, Lígia, El-Sharif, Hazim F., Salles, Maiara O., Boehm, Ryan D., Narayan, Roger J., Paixão, Thiago R.L.C. and Reddy, Subrayal M

1   **MIP-based Electrochemical Protein Profiling**

2

3   Lígia Bueno #[(1)], Hazim F. El-Sharif #[(2)], Maiara O. Salles #[(1)], Ryan D. Boehm[(3)],

4   Roger J. Narayan[(3)], Thiago R. L. C. Paixão[(1)] and Subrayal M. Reddy[(2*)]

5

6   [1] Instituto de Quimica, Universidade de São Paulo, Avenida Professor Lineu Prestes,

7   748 – São Paulo – SP, Brasil.

8   [2] Department of Chemistry, FEPS, University of Surrey, Guildford, UK, GU2 7XH.

9   [3] Joint Departments of Biomedical Engineering, University of North Carolina,

10   Raleigh, USA.

11

12   # These authors contributed equally to this work (co-first authorship)

13

14   **Corresponding Author:** Tel: +44 (0) 1483686396, s.reddy@surrey.ac.uk

15   **Graphical Abstract**

Bovine haemoglobin (BHb)

Polymeric Layer (MIP/NIP)

Cavities

Equine myoglobin (EMb)

Cytochrome C (Cyt C)

Chemometrics

Cyclic Voltammetry

Transducer

Discrimination

Bovine serum albumin (BSA)
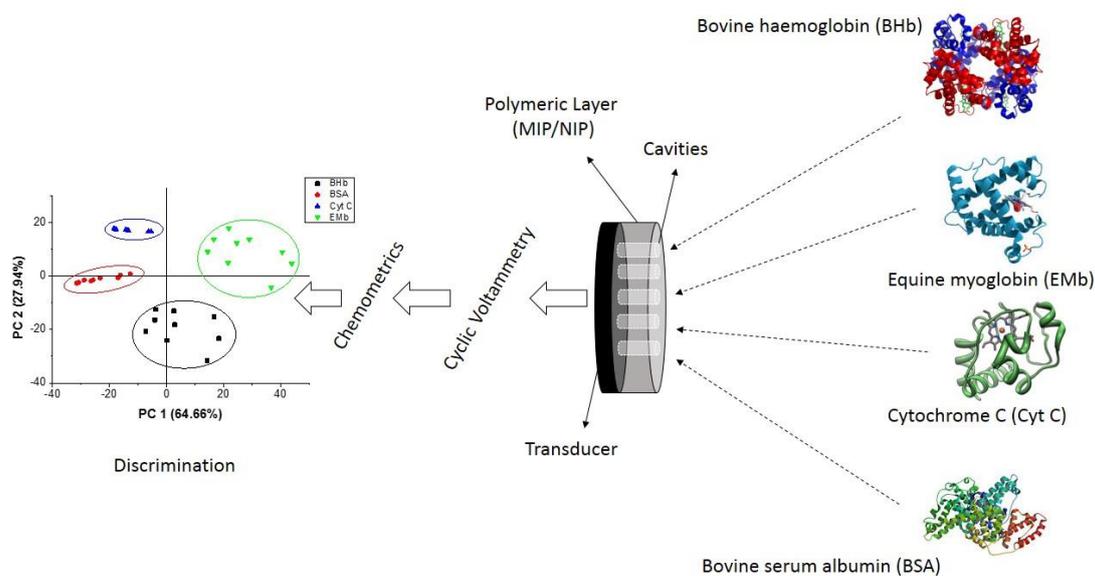
16

17   **Highlights**

18   • Electrochemical MIP-based biosensor fabricated for rapid protein detection.

19   • We report the coupling of electrochemical and pattern recognition techniques.

20   • Selective synthetic MIP recognition of a range of bio-significant proteins.

21   • Protein fingerprint profiling by principal component analysis

22   • Faster detection rates at lower concentrations.

23

24 **Abstract**

25 We present the development of an electrochemical biosensor based on modified

26 glassy carbon (GC) electrodes using hydrogel-based molecularly imprinted polymers

27 (MIPs) has been fabricated for protein detection. The coupling of pattern recognition

28 techniques via principal component analysis (PCA) has resulted in unique protein

29 fingerprints for corresponding protein templates, allowing for MIP-based protein

30 profiling. Polyacrylamide MIPs for memory imprinting of bovine haemoglobin

31 (BHb), equine myoglobin (EMb), cytochrome C (Cyt C), and bovine serum albumin

32 (BSA), alongside a non-imprinted polymer (NIP) control, were

33 spectrophotometrically, and electrochemically characterised using modified GC

34 electrodes. Rebinding capacities (Q) were revealed to be higher for larger proteins

35 (BHb and BSA, $Q \approx 4.5$) while (EMb and Cyt C, $Q \approx 2.5$). Electrochemical results

36 show that due to the selective nature of MIPs, protein arrival at the electrode via

37 diffusion is delayed, in comparison to a NIP, by attractive selective interactions with

38 exposed MIP cavities. However, at lower concentrations such discriminations are

39 difficult due to low levels of MIP rebinding. PCA loading plots revealed 5 variables

40 responsible for the separation of the proteins; E_p, I_p, $E_{1/2}$, $I_{at -0.8 V}$, $\Delta I_{decay peak current to -0.8}$

41 $_V$. Statistical symmetric measures of agreement using Cohen's kappa coefficient (κ)

42 were revealed to be 63% for bare GC, 96% for NIP and 100% for MIP. Therefore, our

43 results show that with the use of PCA such discriminations are achievable, also with

44 the advantage of faster detection rates. The possibilities for this MIP technology once

45 fully developed are vast, including uses in bio-sample clean-up or selective extraction,

46 replacement of biological antibodies in immunoassays, as well as biosensors for

47 medicine, food and the environment.

48

52

53   **1. Introduction**

54   Molecularly imprinted polymers (MIPs) are rapidly becoming viable

55   alternatives to natural antibodies for sensor technology [1-4]. MIPs offer many

56   advantages in terms of shelf-life, stability, robustness, cost, and ease of preparation

57   [5]. While biological antibodies are routinely used in diagnostic tests and are able to

58   give precise results, they are notably unstable and require lengthy procedures to grow,

59   isolate, and treat before they can be used; ethical issues surrounding the use of animal-

60   based antibodies are also a common drawback [6].

61   Over the years molecular imprinting has become an effective method for

62   imprinting highly specific and selective recognition sites in synthetic polymers [7,8].

63   As such, MIPs have been regarded as 'antibody mimics' and have shown clear

64   advantages over actual antibodies for sensor technology as they are highly cross-

65   linked, intrinsically stable, robust, and have potential use in extreme environments [9].

66   However, in the imprinting community, bio-macromolecules such as proteins present

67   a variety of challenges and successful imprints are highly sought after. Proteins are

68   relatively labile and have changeable conformations that are sensitive to various

69   factors (e.g., solvent environments, pH and temperature) [7,10-12]. Moreover, a large

70   number of proteins are vital markers; for example, in the case of haemoglobin,

71   mutations in genes that encode for the protein's subunits can result in hereditary

72   diseases such as *sickle cell anaemia, thalassaemia,* and *haemoglobinopathies* [1].

73   However, protein-detecting arrays remain under-developed due to the lack of highly

74 selective and specific binding agents that interact with protein surfaces through

75 complementary interactions [13]. It is therefore imperative to develop new

76 methodologies based on protein detection for applications in proteomics, medical

77 diagnostics, and even pathogen detection [13].

78   Differential receptor arrays, that in nature routinely conduct pattern-based

79 recognition, have already been artificially constructed using synthetic

80 receptors/transducers and could provide a possible solution. Such devices have been

81 labelled as electronic noses for smell recognition and electronic tongues for taste

82 recognition. These synthetic receptors/transducers or sensors have low selectivity and

83 consequently exhibit over-lapping signals for different species, providing a fingerprint

84 of a sample that could be used for qualitative discrimination [14]. The operation of

85 these electronic devices uses a concept of the human tongue and nose known as global

86 selectivity [15], in which the biological system does not identify a particular substance

87 but brings together all of the extracted information into patterns that the brain

88 decodes. An electronic sensor that works in a similar way is a chememotric tool e.g.,

89 principal component analysis (PCA). These tools decode complex information and

90 classify standards for recognition [16-18]. Takeuchi et al. previously applied the

91 electronic tongue strategy to the molecular recognition of proteins by using imprinted

92 acrylic acid (AA) and 2-dimethylaminoethyl methacrylate (DMA) polymers [19,20].

93 Three-dimensional PCA scores of the binding data described by Takeuchi et al.

94 revealed that a clear protein distinction was possible and that protein-imprinted

95 polymer arrays can be applied to protein profiling by pattern analysis of binding

96 activity for each polymer [19-21]. PCA has also been used in conjunction with

97 electrochemical methods such as cyclic voltammetry [16,17,22-25]. An attractive

98   approach for the development of biochemical sensors would be the integration of

99   smart materials (e.g., MIPs) with said electrochemical techniques

100   This paper demonstrates the use of pattern recognition techniques to uniquely

101   identify fingerprint profiles for four different proteins by coupling electrochemical

102   sensor strategies with hydrogel-based MIPs. The four proteins chosen were on the

103   basis of their different biological roles, sizes, and electrochemical activities. Bovine

104   hemoglobin (BHb, 64.5 kda) well known for its function in the vascular system as a

105   carrier of oxygen, also in aiding the transport of carbon dioxide and regulating blood

106   pH [26]. Both BHb and EMb (17.5 kda) exhibit well-known electrochemical

107   behaviour [1,24,27,28]. Cytochrome complex (Cyt C, 12.5 kda) is an essential

108   component of the electron transport chain but exhibits a lack of oxygen binding,

109   despite being an iron-containing metalloprotein that is capable of undergoing

110   oxidation and reduction. Bovine serum albumin (BSA, MW 66.0 kDa) is a non-

111   metalloprotein with similar molecular weight to BHb, and serves to test the selectivity

112   of the BHb-MIP to BSA compared to template BHb.

113   Our results demonstrate sensitivity and selectivity; if such devices can be

114   further optimised for MIP parameters, then perhaps these MIP-based strategies can

115   offer viable methods for the characterisation of proteins. With the aid of inexpensive

116   synthetic smart material hydrogel MIPs, new biosensor platforms for rapid screening,

117   diagnosis, and monitoring of a variety of disorders can be readily developed within

118   the years to come [8,29].

119

120   **2. Materials and methods**

121   **2.1 Materials**

122   Acrylamide (AA), N,N-methylenebisacrylamide (bis-AA), ammonium

123   persulphate (APS), N,N,N,N-tetramethylethyldiamine (TEMED), sodium dodecyl-

124   sulphate (SDS), glacial acetic acid (AcOH), phosphate buffered saline (PBS) tablets

125   (137 mmol L^{-1} NaCl; 27 mmol L^{-1} KCl; 10 mmol L^{-1} Na_2HPO_4; 1.76 mmol L^{-1}

126   KH_2PO_4), methyl viologen,   bovine haemoglobin (BHb), bovine serum albumin

127   (BSA), cytochrome C (Cyt C), and equine heart myoglobin (EMb) were all purchased

128   from Sigma-Aldrich (Poole, UK). Sieves (75µm) were purchased from Inoxia Ltd.

129   (Guildford, UK). Polycarbonate membranes 25 mm in diameter, 0.8 µm pore size

130   were purchased from Osmonic Inc., Minnetonka, USA.

131

132   **2.2 Hydrogel production**

133   Hydrogel MIPs for BHb, EMb, Cyt C and BSA were synthesised by separately

134   dissolving AA (54 mg) and bis-AA as cross-linker (6 mg) along with template protein

135   (12 mg) in 960 µL of MilliQ water. The solutions were purged with nitrogen for 5

136   minutes, followed by an addition of 20 µL of a 10% (w/v) APS solution and 20 µL of

137   a 5% (v/v) TEMED solution. Polymerisation occurred at room temperature (~22 C^0),

138   giving final total gel densities (%T) of 6 %T, AA/bis-AA (w/v) and crosslinking

139   densities (%C) of 10 %C (9:1, w/w). For every MIP created, a control non-imprinted

140   polymer (NIP) was prepared in an identical manner but in the absence of protein.

141

142   **2.3 Hydrogel conditioning**

143   After polymerization, the gels were granulated separately using a 75 µm sieve.

144   Of the resulting gels, 500 mg were conditioned by washing with five 1 mL volumes of

145   150 mmol L^{-1} PBS buffer (pH 7.4). This was followed by five 1 mL volumes of a

146   10% (w/v):10% (v/v) SDS:AcOH (pH 2.8). A further five 1 mL washes of 150 mmol

147 L^{-1} PBS buffer (pH 7.4) were conducted to remove any residual SDS:AcOH eluent

148 and equilibrate the gels. Each conditioning step was followed by a centrifugation

149 using an Eppendorf mini-spin plus centrifuge (Fisher Scientific, Loughborough, UK)

150 for 3 minutes at 6000 rpm (RCF: 2419 x g). All supernatants were collected for

151 analysis by spectrophotometry to verify the extent of template removal. It should be

152 noted that the last water wash and SDS:AcOH eluent fractions were not observed to

153 contain any protein. Therefore we are confident that any remaining template protein

154 within the MIPs did not continue to leach out during future studies.

155

156 **2.4 Hydrogel characterization**

157 The rebinding efficiency of the MIPs and NIPs produced were characterized

158 using a UV mini-1240 CE spectrophotometer (Shimadzu Europa, Milton Keynes,

159 UK). After elution washing of the polymers MIP and NIP (500 mg) were treated with

160 3 mg/ml of protein in an eppendorf and polymer/protein solution mixed on a rotary

161 vortex mixer for 5 minutes followed by centrifugation. The supernatant was removed

162 and protein concentration measured spectrophotometrically (at 404 nm for BHb; 280

163 nm for BSA, 408 nm for Mb and 402 nm for Cyt C). Protein loaded MIPs and NIPs

164 were then washed with five sequential washes of water (1ml each) and the washes

165 combined. Again the absorbance of the washes was also taken. All protein

166 unaccounted for at this stage was deemed to be selectively bound to the MIP or NIP

167 and determined by subtraction of the protein levels in supernatants (after loading and

168 water washing) from the initial load. Optical microscope images of granulated and

169 washed MIPs and NIPs were also taken.

170

171 **2.5 Electrochemical analysis**

172   Glassy carbon (GC) working electrode surfaces were individually modified

173   with a 20 mg conditioned hydrogel layer of each: NIP, BHb MIP, Cyt C MIP, BSA

174   MIP, and EMb MIP. The layer was kept in place by a polycarbonate membrane (0.8

175   µm) placed over the modified electrode surface and held down with the aid of a

176   rubber ring. The polycarbonate membrane was chosen because its pores are small

177   enough to retain the gel (75 µm particle size) and, at the same time, large enough to

178   allow protein in solution to diffuse through. The potential range used in all

179   electrochemical measurements was 0.0 to -0.9 V with a scan rate of 100 mV s^{-1}; a

180   Ag/AgCl reference electrode (saturated KCl) and platinum counter electrode

181   connected to an Autolab II potentiostat/galvanostat were used in this study (Utrecht,

182   Netherlands). The modified electrodes were first placed in a solution of PBS (pH 7.4)

183   and SDS 5% (w/v) and analysed after a 20 min period of equilibration. Subsequently,

184   15.4 µmol L^{-1} protein solutions (BHb, BSA, EMb and Cyt C) dissolved in PBS buffer

185   (pH 7.4) and SDS 5% (w/v) were placed independently in the cell and

186   voltammograms were obtained at 10 min intervals for 60 min. It should be noted that

187   protein solutions were stirred between measurements for 3 minutes; GC electrodes

188   were cleaned, polished, and tested with methyl viologen between each new MIP/NIP

189   experiment. Cyclic voltammograms using bare GC electrodes were also recorded for

190   the PBS (pH 7.4) and SDS 5% (w/v) buffer solution and for the 15.4 µmol L^{-1} protein

191   solutions (BHb, BSA, EMb and Cyt C) dissolved in PBS buffer (pH 7.4) and SDS 5%

192   (w/v).

193

194   **2.6 Principal component analysis**

195   Principal component analysis (PCA) and hierarchical cluster analysis (HCA)

196   were performed in Statistica 11.0 (StatSoft Inc., Tulsa, USA). The analysis was

197   carried out using voltammetric current density values without any previously pre-

198   processing and scaling from bare GC or modified GC electrodes as input. PCA was

199   used to reduce the large data sets to 2D plots, which can be easily used to discriminate

200   protein samples. All voltammetric curves were recorded three times for each sample

201   in a random order using a clean bare GC or a new modified GC electrode surface.

202

203   **3. Results and discussion**

204   **3.1 Characterisation**

205   Figure 1A and 1B show the optical microscope images of granulated and

206   washed BHb MIPs and NIPs. The MIPs appear denser than the NIPs due to the light

207   contrast apparent from protein which is still locked in the bulk of the MIP. It is also

208   evident that the MIP particles form larger agglomerates with each other compared

209   with the NIP. This is because there is still surface entrapped protein in the MIP

210   particles which is attracted to more surface entrapped protein within other MIP

211   particles. This is not observed with the NIP.

212   The molecular imprinting effect is characterised by the rebinding capacity (Q)

213   of protein to the gel polymer (mg/g) exhibited by the protein-specific MIP and the

214   control NIP, and is calculated using Eq. (1), where C_i and C_r are the initial protein and

215   the recovered protein concentrations (mg/ml) respectively (which specifies the

216   specific protein bound within the gel), V is the volume of the initial solution (ml), and

217   g is the mass of the gel polymers (g).

218     $$Q = [C_i - C_r] \, V/g \qquad (1)$$

219   Figure 1C shows the rebinding capacities for each protein studied. As

220   expected, the MIP exhibited superior selective binding of the target protein compared

221   with the NIP with a typical selectivity ratio of 10:1. Interestingly, the binding capacity

222 is highest for BHb-MIP$_{polyAA}$ while both EMb-MIP$_{polyAA}$ and BCat- MIP$_{polyAA}$ exhibit

223 the lowest binding capacity. It has previously been observed that with smaller size

224 proteins a higher crosslinking density is necessary; the opposite is also true for larger

225 proteins [12,30]. Since the crosslinking density remained the same (10% by weight),

226 the low MIP affinities for BCat and EMb can be attributed to the fact that fewer

227 cavities were imprinted due too high, and too low of a crosslinking density

228 respectively.

229

230 **3.2 Electrochemical analysis**

231 *3.2 .1 Glassy carbon (GC) profiling*

232   Metallo-proteins are expected to produce an electrochemical signal because of

233 their metal-containing haem active centres in the protein molecules. However, the

234 extended three-dimensional structure of proteins results in the inaccessibility of the

235 electroactive iron centres. It can therefore be difficult for metallo-proteins to undergo

236 heterogeneous electron transfer; as a result, no detectable current appears at

237 conventional electrodes [1,4]. However, conformational changes due to partial or

238 complete protein denaturation, can allow haem groups to become accessible to a

239 subjacent electrode and be electrochemically reduced at GC electrodes via promotion

240 of electrocatalytic reduction of nascent oxygen [1]. For example, conformational or

241 structural changes in oxyhaemoglobin (Hb) complexes can be induced upon

242 denaturation in the presence of sodium dodecylsulphate (SDS) denaturant [1,11,31].

243   With this in mind, we attempted to evaluate the possibility to discriminate the

244 proteins using cyclic voltammetric information extracted from bare GC electrodes in

245 the presence of an SDS surfactant in solution. Cyclic voltammograms were recorded

246 in the presence of the four proteins that were studied at 15.4 µmol L^{-1} (including one

247 non-metalloprotein as a control; BHb - 1 mg mL^{-1}, BSA - 0.98 mg mL^{-1}, EMb - 0.26

248 mg mL^{-1}, and Cyt C - 0.185 mg mL^{-1}) in a solution containing PBS buffer (pH 7.4)

249 and 5% SDS (w/v) (Figure 2A). In the presence of Cyt C and BSA, the cathodic

250 reduction signal of dissolved oxygen in solution could be seen (reduction peak at -0.6

251 V). The fact that the peak was due to dissolved oxygen was confirmed by bubbling

252 Ar in the latter protein solutions, which consequently led to depletion of the oxygen

253 reduction peak (results not shown). In the presence of BHb and EMb, a shift in the

254 peak reduction potential towards a less negative potential was observed, indicating an

255 iron centre-dependent electrocatalytic process for the oxygen reduction reaction at the

256 surface of the electrode. This effect was not observed in the absence of SDS, and is

257 therefore due to a probable SDS–induced change in the haemoglobin and myoglobin

258 structural conformation exposing the Fe(III) centre by partial denaturation. The

259 partial denaturation is induced only by SDS where at 5% (w/v) the CMC is reached.

260 Full denaturation however, requires a combination of SDS surfactant and an acid in

261 order to protonate the protein and hence be further attracted to and unravelled by

262 negatively charged SDS micelles [31]. With this modification, the reduction of the

263 oxygen does not directly happen at the electrode surface; the Fe(III) is reduced to

264 Fe(II) at the electrode surface and the oxygen reduction is subsequently

265 electrocatalysed by the oxidation of Fe(II) back to Fe(III).

266 Using hierarchical cluster analysis (HCA) the qualitative discrimination of the

267 proteins on the GC electrode was performed and data were analysed for their

268 discrimination and compiled as number of cluster recognition (Figure 2B). The results

269 reveal that a slight degree of separation between the proteins that, in solution, exhibit

270 and do not exhibit a shift in the peak reduction potential of the oxygen

271 electrochemical process, as clearly observed in the voltammetric profile. However,

272　further evaluation of the recognized sample similarities shows that the model using

273　data extract with a bare electrode was unable to clearly discriminate individual

274　proteins inside the groups of protein clusters.

275

276　*3.2.2 Hydrogel profiling*

277　　　　That the MIP can detect partially denatured protein is of significance to the

278　exploitation of this electrochemical technique in protein discrimination. Indeed

279　Kryscico *et al.* recently demonstrated using CD spectroscopy that during the

280　imprinting process, some of the protein undergoes conformational changes and is

281　partially denatured [32,33]. The MIPs therefore are imprinted with both native as well

282　as partially denatured protein. The MIPs and NIPs were therefore analysed

283　electrochemically with SDS treated protein to give partially denatured protein.

284　　　　Considering the selective nature of MIPs, protein arrival at the electrode

285　surface via diffusion should be delayed by the MIP due to attractive selective

286　interactions with exposed cavities [1]. With this in mind, GC electrode surfaces were

287　individually modified with a conditioned hydrogel layer (20 mg) of BHb MIP, EMb

288　MIP, Cyc C MIP, and BSA MIP.

289　　　　To ensure the successful elution of protein from the MIP (and thus confirming

290　the presence of selective cavities through conditioning), BHb MIPs at different stages

291　were tested electrochemically on the electrode. Figure 3A characterizes the cyclic

292　voltammograms for freshly prepared MIP (with BHb still in the cavities; referred to as

293　MIP1), the same MIP washed to remove protein (referred to as MIP2) and also NIP.

294　The results clearly demonstrate that the MIP loaded with protein exhibits similar

295　electrochemistry to the BHb solution in Figure 2A. The reduction peak observed at

296　around -0.4V is the iron mediated reduction of oxygen. This suggests that the GC

297   electrode is able to detect the protein at the surface due to the 'un-eluted' MIP's

298   presence and concurred with previously reported electrochemical MIP studies [1].

299   Conversely, when protein is not present in either the MIP or the NIP, the

300   electrochemistry (reduction peak at -0.6 V) reverts to direct electrochemical reduction

301   of dissolved oxygen.

302   Protein diffusion through MIP and NIP layers was initially studied at 154 and

303   15.4 µmol L^{-1}. Whereas the NIP response time remained constant at 10 min for all

304   protein concentrations, we found that the MIP response time decreases from our

305   previously reported 40 min [1] to 10 min at low protein concentrations. Figure 3B

306   illustrates the resulting voltammograms for 0 and 10 minutes of BHb exposure at 15.4

307   µmol L^{-1} using a modified BHb-MIP layer (20 mg). It can be seen that a shift in the

308   peak reduction potential for the oxygen reduction was observed after only 10 min of

309   BHb exposure. Therefore, both MIP and NIP share the same reduced response time at

310   lower concentrations. This result suggests that the template protein exhibits little

311   interaction with the MIP cavities at the lower concentrations, which is associated with

312   a less tortuous path to the electrode. It could be that at low protein concentrations we

313   observe extensive protein denaturation in the presence of SDS and therefore there is

314   little or no interaction between denatured protein and the mixed population of MIP

315   cavities for native and partially denatured protein.

316   Another possibility is that the 'template' forms a mixed population of free and

317   clustered proteins when the template is imprinted at a very high concentration (12 mg

318   mL^{-1}). The resultant population of imprinted sites would therefore contain some

319   cavities that are associated with protein clusters. This phenomenon is supported by

320   our previous work [34,35], where force spectroscopy analysis of MIPs suggested that

321   the cavities accommodated an agglomeration of template protein molecules rather

322 than just a single molecule. It is therefore possible that the solution phase represents a

323 more dispersed protein population compared with the original imprinted template

324 population for rebinding protein at low concentrations. If the cavities only respond to

325 a critical number of protein molecules in a given arrangement, then this could explain

326 why the MIP does not appear to be selective at low protein concentrations.

327 However, although the presence of SDS in solution (5% (w/v)) allows for

328 protein detection at the electrode by iron exposure, it also implies that MIP

329 recognition within the specific cavities may technically not be able to rebind the

330 partially denatured and unfolded protein structures due to an altered size and shape. In

331 light of this, recent studies have shown that when imprinting a mixture of stable and

332 partially denatured proteins are present [9,32,33].Therefore it is still possible that the

333 MIPs can function as a recognition element and rebind a small percentage of the

334 heterogeneous protein configurations.

335 In order to confirm these assumptions and elucidate the hypothesis that MIP

336 cavities undergo an electrochemical discrimination of their template proteins,

337 individually modified GC electrodes with all four hydrogel MIP layers were

338 separately tested across all four proteins. Cyclic voltammograms for all MIP were

339 recorded in a solution containing PBS (pH 7.4), SDS 5% (w/v), and 15.4 µmol L^{-1} of

340 the four proteins for different times of protein exposure (0-60 minutes). It was noted

341 that the current signal for both BHb and EMb at 15.4 µmol L^{-1} achieved steady state

342 behaviour after 10 minutes, indicating that this time could be used for all further

343 measurements. Therefore, using the voltammetric current density values PCA score

344 plots for each MIP and protein combination were plotted at 10 minutes of protein

345 exposure.

346   Figure 4A illustrates the average PCA score plot for the four MIPs as they all

347   shared the same cluster separation. A clear discrimination and separation (using 92.9

348   % of the original information) of the four proteins clusters at 10 min of protein

349   exposure can be seen. This indicated that MIP cavity interactions could play an

350   important role in the discrimination process. Of the four different clusters, Cyt C and

351   BSA clusters are far less scattered than BHb and EMb clusters. An explanation for

352   this behaviour could be ascribed to the fact that the BHb MIP was selective for both

353   BHb and EMb (which bear similarities in their structure), allowing for them to bind in

354   the MIP cavities and consequently making the diffusion rate less reproducible in the

355   MIP. The separation for Cyt C and BSA can be justified due to their adsorption at GC

356   electrode surfaces, subsequently changing the rate of the oxygen reduction. A change

357   in the peak current and in the current decay from peak current to -0.8 V ($\Delta I_{\text{decay peak}}$

358    $_{\text{current to -0.8 V}}$) for the oxygen reduction was observed for all the experiments with Cyt C

359   and BSA proteins when compared with a blank solution. These adsorption rates of

360   Cyt C and BSA can be related to previously published values [27,36]. It is plausible

361   that this adsorption effect and delayed diffusion due to MIP cavity interactions are

362   responsible for the discrimination process [37]. PCA loading plots revealed the

363   variables responsible for the separation of the proteins; 5 variables could be elected:

364   E_p, I_p, $E_{1/2}$, $I_{\text{at -0.8 V}}$, $\Delta I_{\text{decay peak current to -0.8 V}}$.

365   Thus, the effective diffusion rate of proteins through the composite

366   membranes could be a function of specific and non-specific cavities of the polymeric

367   MIP layer [37]. Therefore, the time of protein diffusion was considered an important

368   parameter for the discrimination process. This indicated that GC electrodes modified

369   with an acrylamide cavity-based MIP could be used as a sensor to discriminate

370   different kinds of proteins at 10 minutes of protein exposure. However, mechanical

371   obstruction of the polymeric layer using a control non-imprinted polymer (NIP) on the

372   GC electrode surface was conducted in order to validate the MIP-protein rebinding

373   profiles. This allows only for the non-specificity of the polymeric layer to be

374   evaluated due to the lack of selective cavities. All discrimination experiments were

375   executed identically as reported using the MIP layers; the only altered variable was

376   the modified NIP layer (20 mg). Unfortunately, PCA plots revealed NIP to have

377   similar protein discrimination (Figure 4B) to that of a MIP at 10 minutes of protein

378   exposure. Therefore only the protein diffusion rate through the polymeric layer could

379   be considered as a possible discriminating factor for the four proteins.

380   A closer look at the PCA data using interpreted HCA data compiled as number

381   of cluster recognition reveals that the four proteins are best profiled using both MIP

382   and NIP layers (Figure 5A and B, respectively) when compared with bare GC

383   electrode (Figure 2B). The symmetric measures between our protein discrimination

384   models, in terms of a percentage measurement of agreement using Cohen's kappa

385   coefficient (κ), are illustrated in Table 1. Since the approx. significance (p) = .000

386   (which actually means $p < .0005$), our κ coefficients are statistically significantly

387   different from zero (63% for bare GC, 96% for NIP and 100% for MIP). Therefore,

388   there is a clear comparison between the behavioural models for protein

389   discrimination.

390   Furthermore, clustering relationships for each of the four proteins are

391   apparent; this phenomenon is especially noticeable in the MIP and NIP PCA plots

392   (Figure 4). It should be noted that in different studies, involving bare GC electrodes,

393   MIP modified GC electrodes or NIP modified GC electrodes, all PCA protein clusters

394   fall into the same pattern recognition, thus providing an overall cohesive protein

395   profile. Each protein retains its own individual cluster within a single quadrant of the

396   PCA plot. Interestingly, our studies illustrate that proteins with a metal center behave

397   similarly; it can clearly be seen that both metalloproteins that exhibit a peak potential

398   shift (BHb and EMb) are on the right half of the vector, while BSA and Cyt C are on

399   the other. Moreover, the smaller sized proteins (EMB ~17.5kDa and Cyt C ~12.5kDa)

400   are on the top half of the plot. This recognition approach could be useful for future

401   protein speciation profiling.

402

403   **4. Conclusions**

404   The proposed electrochemical and PCA coupled method proved to be efficient

405   for discriminating four proteins (BHb, Mb, BSA and Cyt C), indicating that glassy

406   carbon (GC) electrodes modified with either a MIP or NIP layer could be used as a

407   fast sensor to discriminate between different kinds of proteins. At high concentrations,

408   the selective nature and integrity of MIPs delays the protein response and leads to an

409   obvious difference between MIP and NIP performance. At lower concentrations, such

410   discriminations are difficult due to an apparent lack of critical protein agglomeration

411   and/or complete denaturation of protein molecules impeding optimum protein binding

412   within cavities. With the use of PCA, protein discrimination has been achievable at

413   faster detection rates. Our results suggest that PCA could be used to interrogate and

414   discriminate between proteins when hydrogels are integrated to electrochemical

415   sensors.

416

429 **References**

430 [1] S.M. Reddy, G. Sette, Q. Phan, Electrochemical probing of selective haemoglobin

431 binding in hydrogel-based molecularly imprinted polymers, Electrochim. Acta. 56

432 (2011) 9203-9208.

433 [2] H. Chen, Z. Zhang, R. Cai, X. Chen, Y. Liu, W. Rao, S. Yao, Molecularly

434 imprinted electrochemical sensor based on amine group modified graphene covalently

435 linked electrode for 4-nonylphenol detection, Talanta. 115 (2013) 222-227.

436 [3] B. Khadro, C. Sanglar, A. Bonhomme, A. Errachid, N. Jaffrezic-Renault,

437 Molecularly imprinted polymers (MIP) based electrochemical sensor for detection of

438 urea and creatinine, Procedia Engineering. 5 (2010) 371-374.

439 [4] X. Kan, Z. Xing, A. Zhu, Z. Zhao, G. Xu, C. Li, H. Zhou, Molecularly imprinted

440 polymers based electrochemical sensor for bovine hemoglobin recognition, Sensors

441 Actuators B: Chem. 168 (2012) 395-401.

442 [5] S.A. Piletsky, N.W. Turner, P. Laitenberger, Molecularly imprinted polymers in

443 clinical diagnostics—Future potential and existing problems, Med. Eng. Phys. 28

444 (2006) 971-977.

445 [6] V.J.B. Ruigrok, M. Levisson, M.H.M. Eppink, H. Smidt, J. van der Oost,

446 Alternative affinity tools: more attractive than antibodies? Biochem. J. 436 (2011) 1-

447 13.

448 [7] M.E. Byrne, V. Salian, Molecular imprinting within hydrogels II: Progress and

449 analysis of the field, Int. J. Pharm. 364 (2008) 188-212.

450 [8] P.A. Lieberzeit, R. Samardzic, K. Kotova, M. Hussain, MIP Sensors on the Way

451 to Biotech Application: Selectivity and Ruggedness, Procedia Engineering. 47 (2012)

452 534-537.

453 [9] D.R. Kryscio, N.A. Peppas, Critical review and perspective of macromolecularly

454 imprinted polymers, Acta Biomaterialia. 8 (2012) 461-473.

455 [10] S.M. Reddy, D.M. Hawkins, Q.T. Phan, D. Stevenson, K. Warriner, Protein

456 detection using hydrogel-based molecularly imprinted polymers integrated with dual

457 polarisation interferometry, Sensors Actuators B: Chem. 176 (2013) 190-197.

458 [11] E. Verheyen, J.P. Schillemans, M. van Wijk, M. Demeniex, W.E. Hennink, C.F.

459 van Nostrum, Challenges for the effective molecular imprinting of proteins,

460 Biomaterials. 32 (2011) 3008-3020.

461 [12] H.F. El-Sharif, Q.T. Phan, S.M. Reddy, Enhanced selectivity of hydrogel-based

462 molecularly imprinted polymers (HydroMIPs) following buffer conditioning, Anal.

463 Chim. Acta. 809 (2014) 155-161.

464 [13] H.C. Zhou, L. Baldini, J. Hong, A.J. Wilson, A.D. Hamilton, Pattern recognition

465 of proteins based on an array of functionalized porphyrins, J. Am. Chem. Soc. 128

466 (2006) 2421-2425.

467 [14] Y. Vlasov, A. Legin, A. Rudnitskaya, C. Di Natale, A. D'Amico, Nonspecific

468 sensor arrays ("electronic tongue") for chemical analysis of liquids (IUPAC Technical

469 Report), Pure and Applied Chemistry. 77 (2005) 1965-1983.

470 [15] K. Toko, Taste sensor with global selectivity, Materials Science & Engineering

471 C-Biomimetic Materials Sensors and Systems. 4 (1996) 69-82.

472 [16] J. Zeravik, A. Hlavacek, K. Lacina, P. Skládal, State of the Art in the Field of

473 Electronic and Bioelectronic Tongues ? Towards the Analysis of Wines,

474 Electroanalysis. 21 (2009) 2509-2520.

475 [17] E.A. Baldwin, J. Bai, A. Plotto, S. Dea, Electronic Noses and Tongues:

476 Applications for the Food and Pharmaceutical Industries, Sensors. 11 (2011) 4744-

477 4766.

478 [18] C. Baggiani, L. Anfossi, C. Giovannoli, C. Tozzi, Multivariate analysis of the

479 selectivity for a pentachlorophenol-imprinted polymer, Journal of Chromatography B.

480 804 (2004) 31-41.

481 [19] T. Takeuchi, D. Goto, H. Shinmori, Protein profiling by protein imprinted

482 polymer array, Analyst. 132 (2007) 101-103.

483 [20] T. Takeuchi, T. Hishiya, Molecular imprinting of proteins emerging as a tool for

484 protein recognition, Organic & Biomolecular Chemistry. 6 (2008) 2459.

485 [21] K.D. Shimizu, C.J. Stephenson, Molecularly imprinted polymer sensor arrays,

486 Curr. Opin. Chem. Biol. 14 (2010) 743-750.

487 [22] T.R.L.C. Paixao, M. Bertotti, Fabrication of disposable voltammetric electronic

488 tongues by using Prussian Blue films electrodeposited onto CD-R gold surfaces and

489 recognition of milk adulteration, Sensors and Actuators B-Chemical. 137 (2009) 266-

490 273.

491 [23] M.O. Salles, M. Bertotti, T.R.L.C. Paixao, Use of a gold microelectrode for

492 discrimination of gunshot residues, Sensors and Actuators B-Chemical. 166 (2012)

493 848-852.

494   [24] W. Novakowski, M. Bertotti, T.R.L.C. Paixao, Use of copper and gold electrodes

495   as sensitive elements for fabrication of an electronic tongue: Discrimination of wines

496   and whiskies, Microchemical Journal. 99 (2011) 145-151.

497   [25] L. Bueno, R.L.C. Paixão Thiago, A Single Platinum Microelectrode for

498   Identifying Soft Drink Samples, International Journal of Electrochemistry. 2012

499   (2012) 1-5.

500   [26] Q. Gai, F. Qu, Y. Zhang, The Preparation of BHb-Molecularly Imprinted Gel

501   Polymers and Its Selectivity Comparison to BHb and BSA, Sep. Sci. Technol. 45

502   (2010) 2394-2399.

503   [27] S. Boussaad, N.J. Tao, R. Zhang, T. Hopson, L.A. Nagahara, In situ detection of

504   cytochrome c adsorption with single walled carbon nanotube device, Chem. Commun.

505   0 (2003) 1502-1503.

506   [28] S. Wu, W. Tan, H. Xu, Protein molecularly imprinted polyacrylamide membrane:

507   for hemoglobin sensing, Analyst. 135 (2010) 2523-2527.

508   [29] M.J. Whitcombe, I. Chianella, L. Larcombe, S.A. Piletsky, J. Noble, R. Porter, A.

509   Horgan, The rational development of molecularly imprinted polymer-based sensors

510   for protein detection, Chem. Soc. Rev. 40 (2011) 1547-1571.

511   [30] D.E. Hansen, Recent developments in the molecular imprinting of proteins,

512   Biomaterials. 28 (2007) 4178-4191.

513   [31] D.M. Hawkins, D. Stevenson, S.M. Reddy, Investigation of protein imprinting in

514   hydrogel-based molecularly imprinted polymers (HydroMIPs), Anal. Chim. Acta. 542

515   (2005) 61-65.

516   [32] D.R. Kryscio, M.Q. Fleming, N.A. Peppas, Conformational studies of common

517   protein templates in macromolecularly imprinted polymers, Biomed. Microdevices.

518   14 (2012) 679-687.

519   [33] D.R. Kryscio, M.Q. Fleming, N.A. Peppas, Protein Conformational Studies for

520   Macromolecularly Imprinted Polymers, Macromolecular Bioscience. 12 (2012) 1137-

521   1144.

522   [34] E. Saridakis, S. Khurshid, L. Govada, Q. Phan, D. Hawkins, G.V. Crichlow, E.

523   Lolis, S.M. Reddy, N.E. Chayen, Protein crystallization facilitated by molecularly

524   imprinted polymers, Proceedings of the National Academy of Sciences. 108 (2011)

525   11081-11086.

526   [35] H. EL-Sharif, D.M. Hawkins, D. Stevenson, S.M. Reddy, Determination of

527   protein binding affinities within hydrogel-based molecularly imprinted polymers

528   (HydroMIPs), Phys. Chem. Chem. Phys. 16 (2014) 15483-15489.

529   [36] X. Zhao, R. Liu, Z. Chi, Y. Teng, P. Qin, New Insights into the Behavior of

530   Bovine Serum Albumin Adsorbed onto Carbon Nanotubes: Comprehensive

531   Spectroscopic Studies, J Phys Chem B. 114 (2010) 5625-5631.

532   [37] R. Schirhagl, U. Latif, D. Podlipna, H. Blumenstock, F.L. Dickert, Natural and

533   Biomimetic Materials for the Detection of Insulin, Anal. Chem. 84 (2012) 3908-3913.

534

535

536   **Table captions**

537

538   Table 1 - Symmetric Measures; Cohen's kappa coefficient (κ) as a percentage

539   measurement of agreement, asymptotic std. error not assuming the null hypothesis[a],

540   approximate T as the ratio of κ to the asymptotic standard error assuming the null

541   hypothesis[b], and the approximate statistical significance (p).

542

543

Figure captions

545

546 Figure 1 - Microscope imaging of 75µm hydrogel particles: (A) non-imprinted control

547 (NIP); (B) bovine haemoglobin (BHb) imprinted MIP_{polyAA}. (C) Rebinding capacities

548 and imprinting effects of MIP_{polyAA} and NIP_{polyAA} for several biological molecules

549 (bovine haemoglobin (BHb), bovine serum albumin (BSA), myoglobin (Mb),

550 Cytochrom C (Cyt C)). Data represents mean ± S.E.M., $n = 3$.

551

552 Figure 2 – (A) Cyclic voltammograms recorded in PBS (pH 7.4), SDS 5% (w/v), and

553 in the presence of protein in solution (15.4 µmol L^{-1}) (cytochrome C (a), bovine serum

554 albumin (b), equine heart myoglobin (c) and bovine haemoglobin (d)). Scan rate: 100

555 mV s^{-1}. Electrode: bare glassy carbon (GC) electrode. (B) Cluster analysis percentage

556 prediction scores for the four proteins using GC electrodes.

557

558 Figure 3 - Cyclic voltammograms recorded in PBS (pH 7.4), SDS 5% (w/v), and in

559 the presence of BHb in solution (15.4 µmol L^{-1}) at scan rate of 100 mV s^{-1}: (A) Glassy

560 carbon (GC) electrode modified with hydrogel layers of NIP (a), unconditioned BHb-

561 MIP1 (b), conditioned BHb-MIP2 (c) after 0 minutes of protein exposure. (B) Glassy

562 carbon (GC) electrode modified with hydrogel layer of BHb MIP. Measurement made

563 after 0 (a) and 10 (b) minutes of protein exposure.

564

565

566 Figure 4 - PCA score plots: (A) glassy carbon (GC) electrode modified with hydrogel

567 MIP layer, results show the average response of all four different MIPs; (B) glassy

568 carbon (GC) electrode modified with a non-imprinted hydrogel layer. Voltammetric

569   date recorded in PBS (pH 7.4), SDS 5% (w/v), and in the presence of each protein

570   (15.4 µmol L^{-1}). Potential programme employed to record the voltammetric curves

571   used as input to perform PCA: E_i=0.0 V, E_{V1}=-0.9 V, E_f = 0.0 V, and scan rate = 100

572   mV s^{-1}. Measurement made after 10 minutes of protein exposure.

573

574   Figure 5 - Cluster analysis percentage prediction scores for the four proteins; (A) MIP

575   modified GC electrodes, (B) NIP modified GC electrodes.

576

577   Table 1

| Model	κ (%)	Asymp. Std. Error[a]	Approx. T[b]	Approx. Sig. (ρ)
Bare GCE	63%	0.1	6.543	0.00
NIP	96%	0.036	10.018	0.00
Mb MIP	100%	0	10.392	0.00
Cyt C MIP	100%	0	10.392	0.00
BSA MIP	100%	0	10.392	0.00
BHb MIP	96%	0.04	9.414	0.00

578

579
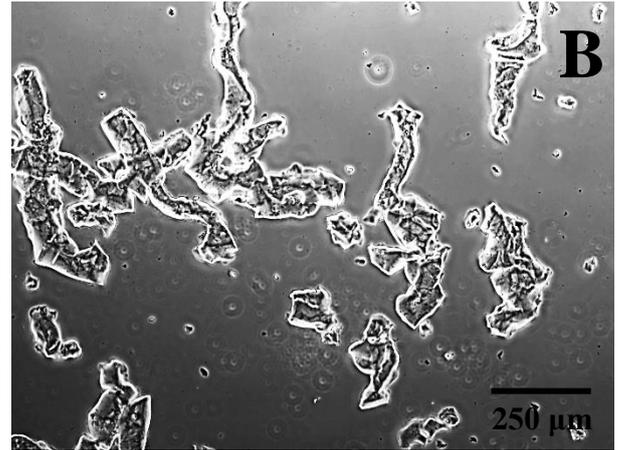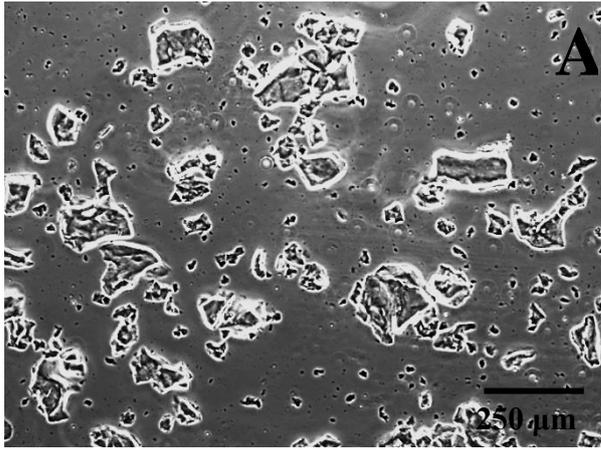
580
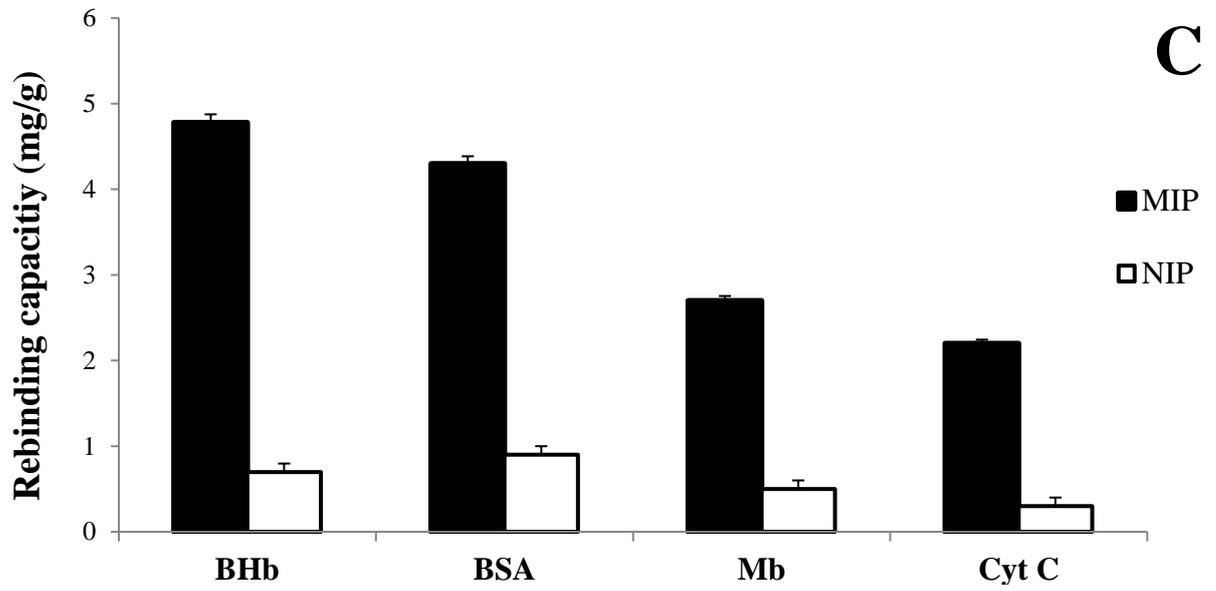
581

582   Figure 1

583
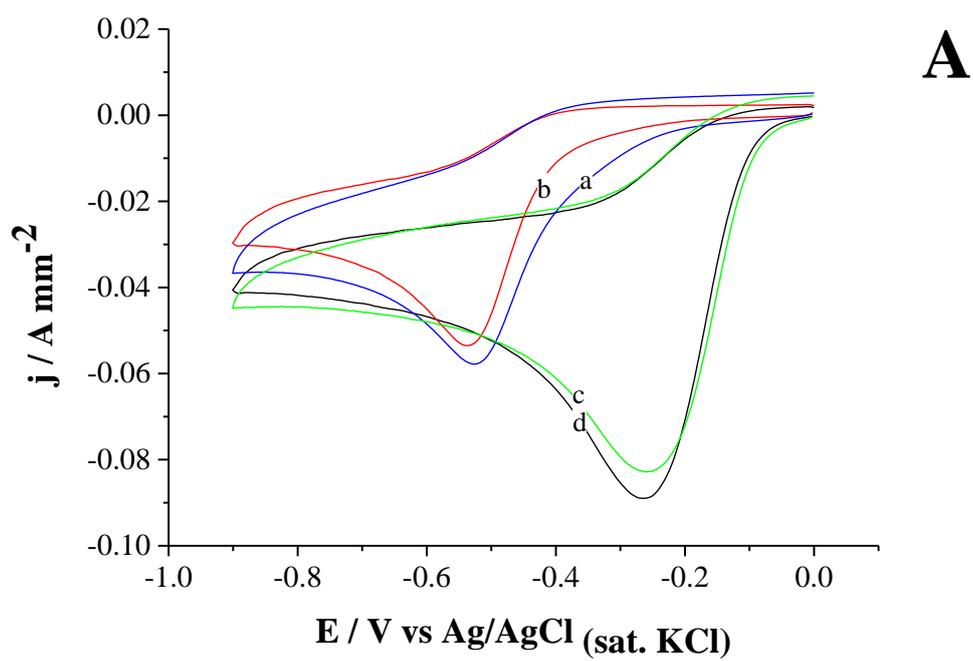
584
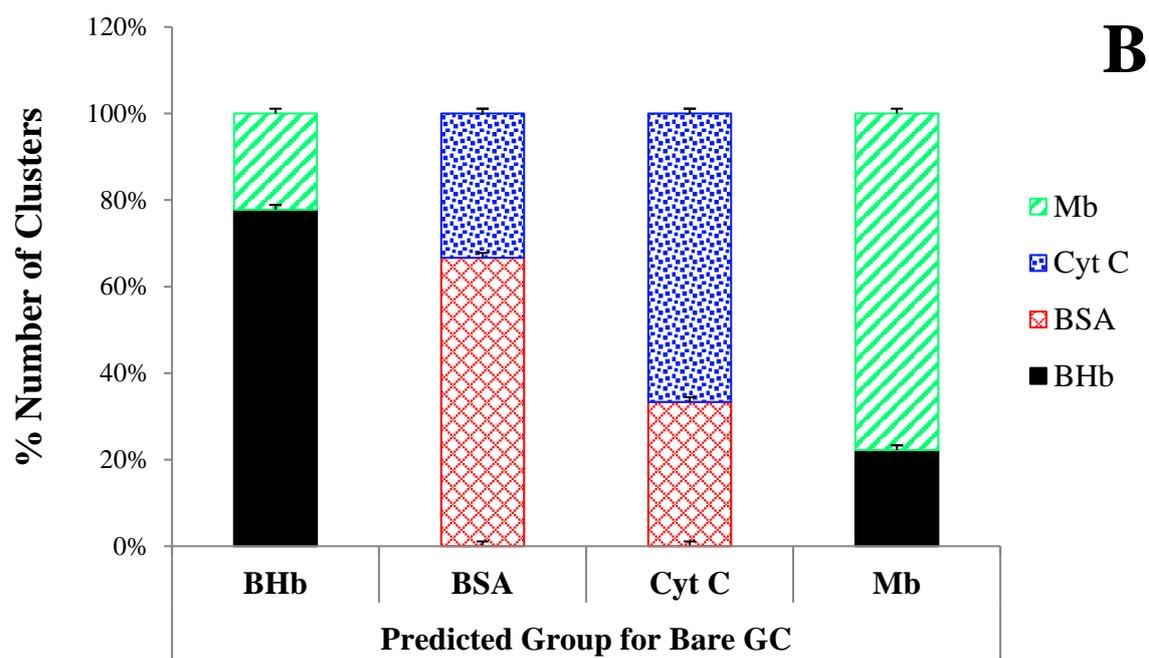
585

586   Figure 2
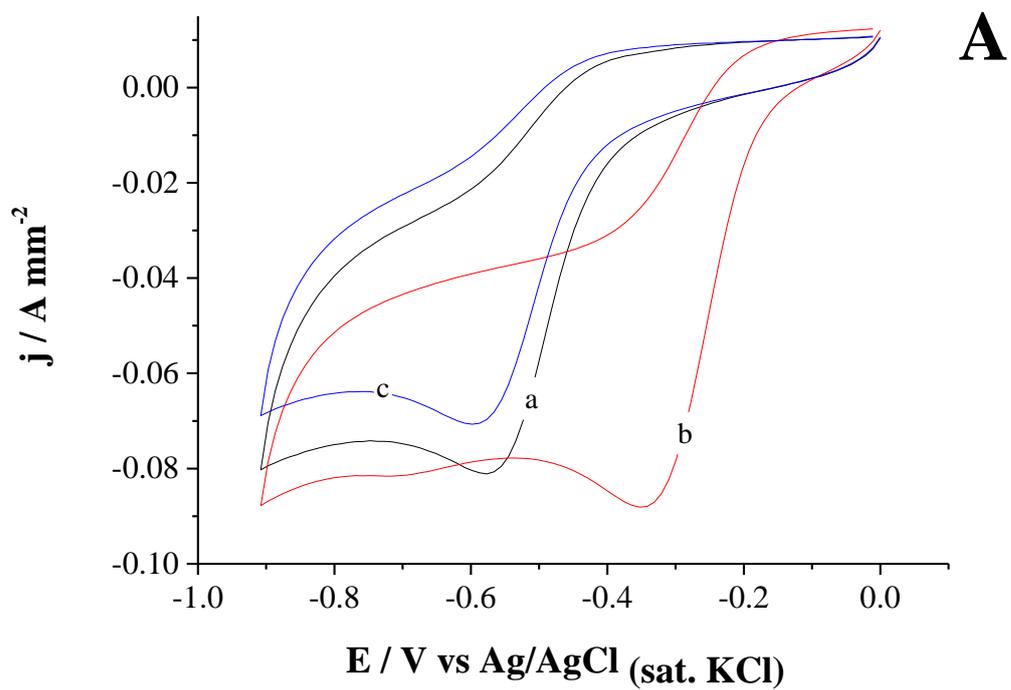
587
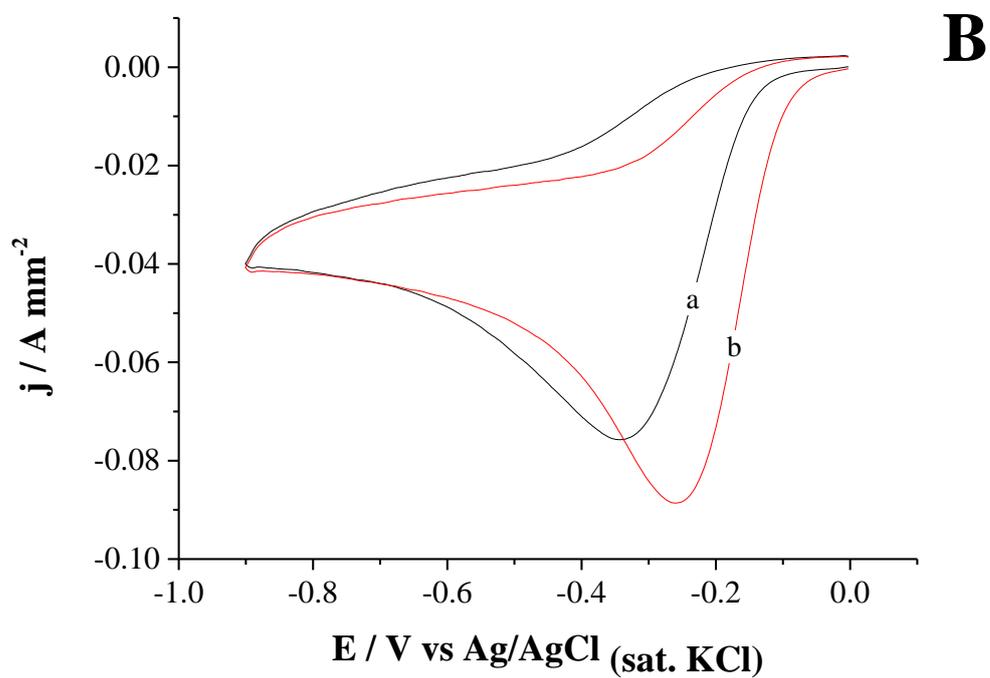
588
589   Figure 3
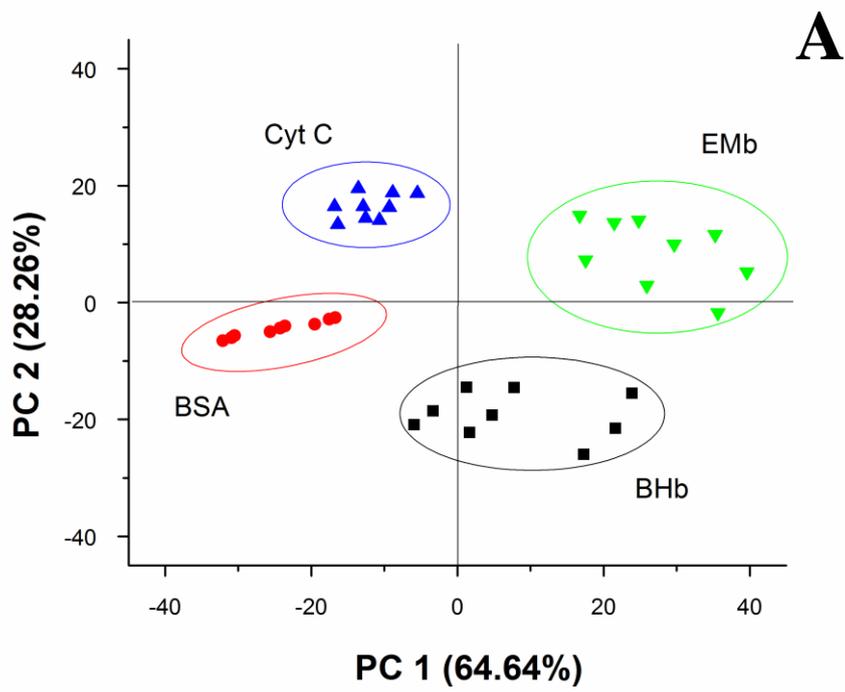
590

591

592   Figure 4
593

A

594

B

595

596

597 Figure 5

598